

Brownian yet non-Gaussian diffusion of a light particle in heavy gas: Lorentz gas based analysis

Fumiaki Nakai^{1,*} and Takashi Uneyama¹

¹*Department of Materials Physics, Graduate School of Engineering,
Nagoya University, Furo-cho, Chikusa, Nagoya 464-8603, Japan*

Non-Gaussian diffusion was recently observed in a gas mixture with mass and fraction contrast [F. Nakai et al, Phys. Rev. E **107**, 014605 (2023)]. The mean square displacement of a minor gas particle with a small mass is linear in time, while the displacement distribution deviates from the Gaussian distribution, which is called the Brownian yet non-Gaussian diffusion. In this work, we theoretically analyze this case where the mass contrast is sufficiently large. Major heavy particles can be interpreted as immobile obstacles, and a minor light particle behaves like a Lorentz gas particle within an intermediate time scale. Despite the similarity between the gas mixture and the conventional Lorentz gas system, the Lorentz gas description cannot fully describe the Brownian yet non-Gaussian diffusion. A successful description can be achieved through an ensemble average of the statistical quantities of the Lorentz gas over the initial speed.

I. INTRODUCTION

Gas diffusion is a classical problem [1–4], and it may be considered to be fully understood nowadays. However, recent work revealed that gas diffusion is not that simple nor fully understood [5]. The authors[5] numerically investigated the diffusion of a light gas particle in gas mixtures with mass and fraction contrast and found that the minor light molecule exhibits Brownian yet non-Gaussian diffusion: the mean square displacement (MSD) is linear in time, while the displacement distribution deviates from the Gaussian distribution. The Brownian yet non-Gaussian diffusion has been widely observed in complex systems with heterogeneous environments and/or conformational degrees of freedom, such as glass-forming liquids [6], polymeric fluids [7, 8], colloidal suspensions [9, 10], biological systems [11–13], and active matters [14, 15]. In contrast to these complex systems, there is no heterogeneity nor internal degrees of freedom in the gas mixture. In the previous work [5], the origin of the non-Gaussian behavior was attributed to the fluctuating diffusivity which arises from a timescale separation between the velocity direction and speed of the minor light particle.

The dynamics of a light particle in heavier particles have often been approximated as the Lorentz gas [4, 16–18], which is composed of a mobile particle and immobile particles. Although Lorentz gas was originally constructed for the dynamics of an electron in metal, later, the model has been regarded as the simple model for the transport phenomena of gas [17] and also for some classical dynamical systems [19, 20]. Various properties of the Lorentz gas including the diffusion coefficient [16, 21] or the relaxation of the velocity [16, 17] are analyzed, and diverse extended models [19, 20, 22] have been extensively studied. Naively, we expect that the diffusion of a light gas particle in the heavy gas particles can be described using Lorentz gas. To the best of the authors' knowledge, the relation between the simple dilute Lorentz gas and diffusion of a light particle in a matrix of heavy gas particles is not clear, and whether the non-Gaussian behavior can be described by the Lorentz gas is not clear, neither.

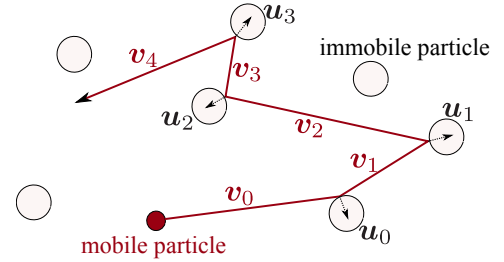


FIG. 1. Binary gas mixture as a Lorentz gas, which consists of a single mobile particle (point mass) in immobile spherical particles. v_i denotes the mobile particle velocity after i -th collision, and u_i is the unit vector from the mobile particle to the colliding immobile particle.

In the current work, we theoretically analyze the diffusion of a light gas particle in heavy gas particles. We employ the dilute random Lorentz gas to describe the Brownian yet non-Gaussian diffusion of a light particle in heavy gas. We first derive analytical expressions for the MSD and the non-Gaussian parameter of the Lorentz gas using the point process [23]. Afterward, we calculate the ensemble average of them over the initial speed, which obeys the Maxwell-Boltzmann distribution. The averaged result quantitatively reproduces the Brownian yet non-Gaussian diffusion of a light and minor gas particle in binary gas mixtures within an intermediate timescale.

II. MODEL

We consider a system that consists of the mobile particle with mass m and size 0 (point mass) in the fixed spherical obstacles with radius σ . Note that we introduce the mass m to analyze the binary gas mixture, although the conventional Lorentz gas model is independent of m . We limit ourselves to the case where the fixed obstacles are dilute. The fixed obstacles are randomly distributed in space, and there is no statistical correlation between different obstacles. We describe the number density of the obstacles as ρ . The mobile particle ballistically moves until it collides with an immobile obstacle. When the mobile particle collides with the obstacle, the velocity of the mobile particle instantaneously changes via the

* nakai.fumiaki.c7@s.mail.nagoya-u.ac.jp

hard-core repulsion potential [4]. If we describe the velocities of the mobile particle before and after the i -th collision as \mathbf{v}_i and \mathbf{v}_{i+1} , they are related as

$$\mathbf{v}_{i+1} = (\mathbf{1} - 2\mathbf{u}_i\mathbf{u}_i) \cdot \mathbf{v}_i \quad (1)$$

where \mathbf{u}_i is the unit vector connecting the mobile particle to the colliding immobile particle, and $\mathbf{1}$ is the unit tensor. See Fig. 1 for a schematic representation of our model. From Eq. (1), the speed of the mobile particle v remains unchanged: $v = |\mathbf{v}_i|$ (for any i). As we mentioned, we consider the dilute obstacle case, and the successive collisions are assumed to be uncorrelated. In this case, the dynamics of the mobile particle can be described as a Markovian stochastic process. If we choose m , v , and $1/\rho\sigma^2$ to define the dimensionless units, there are no parameters in the random dilute Lorentz gas.

The model explained above can be interpreted as an approximate description for a minor and light particle in binary gas mixtures with sufficiently large mass and fraction contrast. In such a binary gas mixture, the heavy particles are not entirely immobile but can move very slowly. This means that the speed of the mobile particle is not exactly constant but just approximately constant at a specific time scale. Later, we will discuss a relation between the Lorentz gas and the gas mixture with mass and fraction contrast.

III. THEORY AND DISCUSSIONS

A. Lorentz Gas

The dynamics of the mobile particle are described using \mathbf{v}_i and t_i , where t_i is the collision time at the i -th collision. Using \mathbf{v}_i and t_i , the position of the mobile particle at the time t after the n -th collision, $\mathbf{r}(n, t)$, can be described as

$$\mathbf{r}(n, t) = \mathbf{v}_n(t - t_n) + \sum_{i=0}^{n-1} \mathbf{v}_i(t_{i+1} - t_i). \quad (2)$$

To describe the dynamics, we require the collision statistics between successive collisions. In the current case, the collision frequency density $f(\mathbf{u})$ for a collision with a direction vector \mathbf{u} thoroughly characterizes the collision statistics. $f(\mathbf{u})$ is obtained from the collision statistics for the binary gas mixture[3, 5] by setting the surrounding gas velocity to be 0:

$$f(\mathbf{u}_i) = \rho\sigma^2 \mathbf{v}_i \cdot \mathbf{u}_i \Theta(\mathbf{v}_i \cdot \mathbf{u}_i), \quad (3)$$

where $\Theta(x)$ is the Heaviside step function. Eq. (3) can be rewritten into a simple form in the spherical coordinates. Without loss of generality, we can take the Cartesian coordinates for \mathbf{v}_i as $\mathbf{v}_i = (0, 0, v)$ and express \mathbf{u}_i as $\mathbf{u}_i = (\sin\theta_i \cos\phi_i, \sin\theta_i \sin\phi_i, \cos\theta_i)$ with $\theta_i \in [0, \pi/2]$ and $\phi_i \in [0, 2\pi]$. Then Eq. (3) reduces to

$$f(\mathbf{u}_i) = \rho\sigma^2 v \cos\theta_i \quad (4)$$

By integrating Eq. (4) over \mathbf{u}_i , we obtain the collision frequency as

$$\int f(\mathbf{u}_i) d\mathbf{u}_i = \frac{v}{\lambda} \quad (5)$$

where $\lambda = 1/\pi\rho\sigma^2$ is the mean free path. Combining Eqs. (4) and (5), we obtain the probability density where the mobile particle collides at \mathbf{u}_i at the time interval $t_{i+1} - t_i$ for a given v , $P(t_{i+1} - t_i, \mathbf{u}_i; v)$ as [5]

$$P(t_{i+1} - t_i, \mathbf{u}_i; v) = f(\mathbf{u}_i) \exp\left[-\frac{v}{\lambda}(t_{i+1} - t_i)\right]. \quad (6)$$

The probability density at time t with the number of collisions n and the speed v can be calculated using Eq. (6):

$$P(\mathbf{r}, \{\mathbf{u}_i\}, \{t_i\}; n, t, v) = \delta[\mathbf{r} - \mathbf{r}(n, t)] \times \prod_{i=0}^n P(t_{i+1} - t_i, \mathbf{u}_i, v). \quad (7)$$

Integrating Eq. (7) over $\{\mathbf{u}_i\}$ and $\{t_i\}$, we have the probability density for \mathbf{r} under given n , t , and v :

$$\begin{aligned} & P(\mathbf{r}; n, t, v) \\ &= \int d\mathbf{v}_0 \int_t^\infty dt_{n+1} \int_0^t dt_n \int_0^{t_n} dt_{n-1} \cdots \int_0^{t_2} dt_1 \\ & \quad \times \int d\mathbf{u}_n \cdots \int d\mathbf{u}_0 P(\mathbf{r}, \{\mathbf{u}_i\}, \{t_i\}; n, t, v) P(\mathbf{v}_0) \\ &= e^{-vt/\lambda} \int d\mathbf{v}_0 \int_0^t dt_n \int_0^{t_n} dt_{n-1} \cdots \int_0^{t_2} dt_1 \\ & \quad \times \int d\mathbf{u}_{n-1} \cdots \int d\mathbf{u}_0 \delta[\mathbf{r} - \mathbf{r}(n, t)] \prod_{i=0}^{n-1} f(\mathbf{u}_i) P(\mathbf{v}_0; v), \end{aligned} \quad (8)$$

where $P(\mathbf{v}_0; v) = \delta(|\mathbf{v}_0| - v)/4\pi v^2$ is the initial velocity distribution of the mobile particle.

To proceed with the calculation, we introduce the characteristic function, $C(\mathbf{k}; n, t, v) = \int d\mathbf{r} e^{i\mathbf{k} \cdot \mathbf{r}} P(\mathbf{r}; n, t, v)$. From Eq. (8), we can calculate $C(\mathbf{k}; n, t, v)$ as

$$\begin{aligned} & C(\mathbf{k}; n, t, v) \\ &= e^{-vt/\lambda} \int d\mathbf{v}_0 \int_0^t dt_n \int_0^{t_n} dt_{n-1} \cdots \int_0^{t_2} dt_1 \\ & \quad \times \int d\mathbf{u}_{n-1} \cdots \int d\mathbf{u}_0 \prod_{i=0}^{n-1} f(\mathbf{u}_i) P(\mathbf{v}_0; v) \\ & \quad \times \exp\left\{i\mathbf{k} \cdot \left[\mathbf{v}_n(t - t_n) + \sum_{i=0}^{n-1} \mathbf{v}_i(t_{i+1} - t_i)\right]\right\}. \end{aligned} \quad (9)$$

Here we consider the Laplace transform of Eq. (9): $\hat{C}(\mathbf{k}; n, s, v) = \mathcal{L}[C(\mathbf{k}; n, \cdot, v)](s) = \int_0^\infty dt e^{-ts} C(\mathbf{k}; n, t, v)$. Then we have

$$\begin{aligned} \hat{C}(\mathbf{k}; n, s, v) &= \int d\mathbf{v}_0 \frac{P(\mathbf{v}_0; v)}{s - i\mathbf{k} \cdot \mathbf{v}_0 + v/\lambda} \\ & \quad \times \prod_{i=0}^{n-1} \int d\mathbf{u}_i \frac{f(\mathbf{u}_i)}{s - i\mathbf{k} \cdot \mathbf{v}_{i+1} + v/\lambda}. \end{aligned} \quad (10)$$

The integrals over \mathbf{v}_0 and $\{\mathbf{u}_i\}$ in Eq (10) can be analytically calculated. The result is

$$\hat{C}(\mathbf{k}; n, s, v) = \frac{\lambda}{v} \left[\frac{1}{k\lambda} \arctan\left(\frac{kv}{s + v/\lambda}\right) \right]^{n+1}, \quad (11)$$

where $k = |\mathbf{k}|$. To obtain the probability density for \mathbf{r} under given s and v , we need to consider all the contributions from different n . This can be easily calculated by taking the summation over n : $\hat{C}(\mathbf{k}; s, v) = \sum_{n=0}^{\infty} \hat{C}(\mathbf{k}; n, s, v)$. From Eq. (11), we have

$$\hat{C}(\mathbf{k}; s, v) = \frac{\arctan\left(\frac{kv}{s + v/\lambda}\right)}{(v/\lambda) \left[k\lambda - \arctan\left(\frac{kv}{s + v/\lambda}\right) \right]}. \quad (12)$$

Eq. (12) corresponds to the Fourier-Laplace transform of the self part of the van Hove correlation function, and thus any quantities which characterize the diffusion behavior can be calculated from Eq. (12). Note that Eq. (12) satisfies the normalization condition of the probability density: $\hat{C}(\mathbf{k}; s, v) = s^{-1}$ at $k = 0$.

The MSD is calculated as the second-order moment for the van Hove correlation function. From Eq. (12), we have the Laplace transform of the MSD under a given v as follows:

$$\begin{aligned} \mathcal{L}[\langle \mathbf{r}^2(\cdot) \rangle_v](s) &= - \frac{\partial^2}{\partial \mathbf{k}^2} \hat{C}(\mathbf{k}; s, v) \Big|_{\mathbf{k}=0} \\ &= \frac{2v^2}{s^2(s + v/\lambda)}, \end{aligned} \quad (13)$$

where $\langle \dots \rangle_v$ denotes the statistical average under a given v . Similarly, the Laplace transform of the fourth-order moment becomes

$$\begin{aligned} \mathcal{L}[\langle \mathbf{r}^4(\cdot) \rangle_v](s) &= \frac{\partial^2}{\partial \mathbf{k}^2} \frac{\partial^2}{\partial \mathbf{k}^2} \hat{C}(\mathbf{k}; s, v) \Big|_{\mathbf{k}=0} \\ &= \frac{8v^4(9s + 5v/\lambda)}{3s^3(s + v/\lambda)^3}. \end{aligned} \quad (14)$$

The inverse Laplace transforms of Eqs. (13) and (14) give

$$\frac{\langle \mathbf{r}^2(t) \rangle_v}{\lambda^2} = 2 \left(-1 + vt/\lambda + e^{-vt/\lambda} \right), \quad (15)$$

$$\begin{aligned} \frac{\langle \mathbf{r}^4(t) \rangle_v}{\lambda^4} &= \frac{4v^2 t^2}{3\lambda^2} \left(5 + 4e^{-vt/\lambda} \right) - \\ &\quad \frac{8vt}{\lambda} \left(2 - e^{-vt/\lambda} \right) + 8 \left(1 - e^{-vt/\lambda} \right). \end{aligned} \quad (16)$$

It is straightforward to show that at the short-time limit ($t \rightarrow 0$) Eqs. (15) and (16) approach $\langle \mathbf{r}^2(t) \rangle_v \rightarrow v^2 t^2$ and $\langle \mathbf{r}^4(t) \rangle_v \rightarrow v^4 t^4$. These reflect the ballistic motion. At the long-time limit $t \rightarrow \infty$, the MSD approaches $\langle \mathbf{r}^2(t) \rangle_v \rightarrow 2v\lambda t$, which corresponds to the normal diffusion. The diffusion coefficient, D , defined as $\langle \mathbf{r}^2(t; v) \rangle = 6Dt$, becomes $D = v\lambda/3$, which is consistent with the well-established result [4] in the gas kinetic theory. From Eqs. (15) and (16), the analytic expression of the non-Gaussian parameter (NGP) under a given v , $\alpha(t; v)$, is calculated to be

$$\begin{aligned} \alpha(t; v) &= \frac{3\langle \mathbf{r}^4(t) \rangle_v}{5\langle \mathbf{r}^2(t) \rangle_v^2} - 1 \\ &= \frac{4e^{-vt/\lambda}(v^2 t^2/\lambda^2 - vt/\lambda + 1) + 1 - 2vt/\lambda - 5e^{-2vt/\lambda}}{5(-1 + vt/\lambda + e^{-vt/\lambda})^2}. \end{aligned} \quad (17)$$

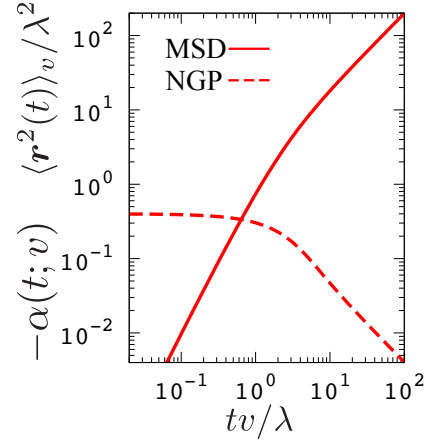


FIG. 2. Theoretical predictions of the scaled mean square displacement (Eq. (15)) and non-Gaussian parameter (Eq. (17)) against reduced time vt/λ for the dilute random Lorentz gas.

Fig. 2 displays the MSD (Eq. (15)) and the absolute value of the NGP (Eq. (17)) (the NGP by Eq. (17) is always negative) of the Lorentz gas. MSD shows simple ballistic and diffusive behaviors at the short and long timescales, respectively. The crossover time is approximately equal to the mean free time, $vt/\lambda \approx 1$. NGP becomes $-2/5$ at the short timescale and approaches 0 at the long time scale. The decay of $-\alpha(t; v)$ starts around $vt/\lambda \approx 1$, where the MSD switches from ballistic motion to normal diffusion. The result that the NGP approaches zero at the long-time scale means that the dynamics of Lorentz gas can be reasonably described by the Gaussian process for $t \gtrsim \lambda/v$. The non-Gaussianity at $t = 0$ originates from the energy conservation of the Lorentz gas. At the short timescale, the mobile particle ballistically moves, and thus NGP reflects the non-Gaussianity of the velocity distribution. We can easily evaluate the NGP at the short-time limit:

$$\alpha(t; v) = \frac{3\langle \mathbf{r}^4 t^4 \rangle_v}{5\langle \mathbf{r}^2 t^2 \rangle_v^2} - 1 = -\frac{2}{5}, \quad (18)$$

which is consistent with the theoretical prediction at the short timescale in Fig. 2.

B. Binary Gas Mixture

The Lorentz gas has often been regarded as the model that describes a light particle in heavy particles. Thus, one may expect that the Brownian yet non-Gaussian diffusion, which is observed for a minor light particle in heavy gas [5], can be predicted from the Lorentz gas model. However, the theoretical result of the random dilute Lorentz gas (Fig. 2) does not exhibit the non-Gaussian diffusion in the normal diffusion regime ($\text{MSD} \propto t$).

This apparent inconsistency between the Lorentz gas model and a binary gas mixture comes from the fact that the speed (or kinetic energy) of a light gas particle in a binary gas mixture can relax at a very long-time scale. This means that the speed of a light particle should not be assumed to be constant

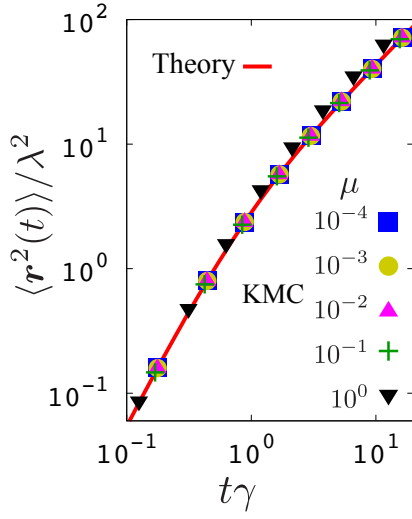


FIG. 3. Theoretical prediction for MSD of binary gas mixtures with different mass ratios. The red curve is the theoretical prediction by Eq. (20), and symbols are the results of KMC simulations[5].

in the long timescale. We need to take the ensemble average for the statistical quantities. The statistical quantities such as the MSD for binary gas mixtures can be interpreted as the statistical average of those for the Lorentz gas over the initial speed. The probability density of the speed of the mobile particle obeys the Maxwell-Boltzmann distribution with the temperature T :

$$P(v) = 4\pi v^2 \left(\frac{m}{2\pi k_B T} \right)^{3/2} \exp\left(-\frac{mv^2}{2k_B T}\right), \quad (19)$$

where k_B is the Boltzmann constant. The ensemble average of the MSD is calculated as

$$\begin{aligned} \frac{\langle r^2(t) \rangle}{\lambda^2} &= \int \frac{\langle r^2(t) \rangle_v}{\lambda^2} P(v) dv \\ &= 2 \left[-1 + \frac{2\gamma t}{\sqrt{\pi}} + (1 + 2\gamma^2 t^2) e^{\gamma^2 t^2} \operatorname{erfc}(\gamma t) \right], \end{aligned} \quad (20)$$

where γ is a characteristic frequency defined as $\gamma = \sqrt{k_B T / 2m} / \lambda$. Fig. 3 displays the prediction for the MSD of a light particle in a binary gas mixture by Eq.(20). For comparison, the mean square displacements of the light particle in heavier particles, calculated from the kinetic Monte Carlo (KMC) simulations [5], are also presented with various mass ratios μ (between light and heavy particles). Our theoretical prediction quantitatively agrees with the MSD from the KMC simulations when the mass ratio is sufficiently small ($\mu \ll 1$).

In a similar manner, the NGP for a binary gas mixture can be analytically calculated. The ensemble average of the

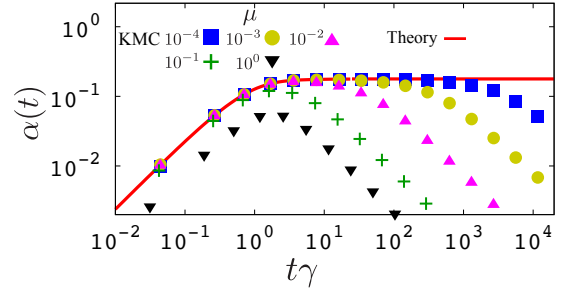


FIG. 4. Theoretical prediction for NGP of binary gas mixtures with different mass ratios. The red curve is the theoretical prediction by Eqs. (20) and (21), and symbols are the results from the KMC simulations[5].

fourth-order moment is obtained as

$$\begin{aligned} \frac{\langle r^4(t) \rangle}{\lambda^4} &= \int \frac{\langle r^4(t) \rangle_v}{\lambda^4} P(v) dv \\ &= \frac{4}{3} \left[6 - \frac{12\gamma t}{\sqrt{\pi}} + 30\gamma^2 t^2 - \frac{56\gamma^3 t^3}{\sqrt{\pi}} - \frac{32\gamma^5 t^5}{\sqrt{\pi}} \right. \\ &\quad \left. - (6 + 24\gamma^2 t^2 - 72\gamma^4 t^4 - 32\gamma^6 t^6) e^{\gamma^2 t^2} \operatorname{erfc}(\gamma t) \right]. \end{aligned} \quad (21)$$

Fig. 4 displays the NGP $\alpha(t)$ calculated from Eqs. (20) and (21). For comparison, the NGPs from the KMC simulations [5] are also shown with various μ . Our theoretical prediction successfully describes the non-Gaussian parameter from the KMC simulation for sufficiently small μ except for the decay of the NGP at the very long time scale. We will discuss this discrepancy later. The NGP by Eqs. (20) and (21) approaches 0 at $t \rightarrow 0$, unlike the case of the Lorentz gas. This reflects the fact that the probability density of the speed of the mobile particle obeys the Maxwell-Boltzmann distribution, which is a Gaussian distribution. At the long-time limit ($t \rightarrow \infty$), the NGP approaches $3\pi/8 - 1$, and this quantity corresponds to the plateau of the NGP from the KMC simulations.

At last, we discuss the self part of the van Hove correlation function $G_s(\mathbf{r}, t)$ at the limit of the long time scale which is sufficiently larger than the mean free time, based on the Lorentz gas model. At the long-time limit in the Lorentz gas ($s \ll v/\lambda$), Eq. (12) reduces to

$$\hat{C}(\mathbf{k}; s, v) \approx \frac{\arctan(k\lambda) - \frac{ks}{k^2 v + v/\lambda^2}}{(v/\lambda) \left[k\lambda - \arctan(k\lambda) + \frac{ks}{k^2 v + v/\lambda^2} \right]}. \quad (22)$$

Its inverse-Laplace-transform is

$$\begin{aligned} C(\mathbf{k}; t, v) &\approx (1 + k^2 \lambda^2) \exp \left[-\frac{(1 + k^2 \lambda^2) [k\lambda - \arctan(k\lambda)] tv}{k\lambda \lambda} \right]. \end{aligned} \quad (23)$$

Here, we should note that Eq. (23) is valid for the long-time scale, $t \gg \lambda/v$. In this timescale, we expect that only the

small wavelength component ($k\lambda \ll 1$) becomes dominant. Then Eq.(23) can be reduced to

$$C(\mathbf{k}; t, v) \approx \exp\left(-\frac{vt\lambda k^2}{3}\right). \quad (24)$$

Eq. (24) is nothing but the characteristic function of the Gaussian distribution. Thus, the van-Hove correlation function of the Lorentz gas for a given speed v at the long-time limit is

$$G(x; t, v) \approx \sqrt{\frac{3}{4\pi v\lambda t}} \exp\left(-\frac{3x^2}{4v\lambda t}\right). \quad (25)$$

From Eqs. (19) and (25), we obtain the van-Hove correlation function for a light gas particle in a binary gas mixture as

$$G(x; t) = \int_0^\infty G(x; t, v)P(v)dv, \quad (26)$$

This formula is the same as obtained phenomenologically in the previous work [5].

As we mentioned, our theoretical prediction for the NGP $\alpha(t)$ converges to a constant value at the long-time limit. Therefore, at least in the theoretical framework shown above, our theory does not predict the Gaussian behavior at the long-time region observed in the KMC simulations. The discrepancy between the theoretical prediction and the KMC data at the long-time limit can be attributed to the lack of speed relaxation in our analysis. The KMC simulations revealed that there are two characteristic relaxation time scales in a binary gas mixture: the direction and speed relaxations [5]. In our analysis, we considered the direction relaxation via hard-core collisions, while the speed relaxation is not explicitly considered. We only assumed that the speed relaxation makes the initial ensemble with the Maxwell-Boltzmann distribution. The speed relaxation affects the long-time dynamics, but it is totally ignored. Therefore, the diffusion coefficient for the particle with a given initial speed v remains constant even at

the long-time limit: $D = v\lambda/3$. This means that the long-time diffusion behavior reflects the initial speed distribution. This is why the NGP does not approach zero even at the long-time limit.

The diffusion coefficient of a light particle in a binary gas mixture fluctuates in time due to speed relaxation. Therefore, if we describe the diffusion of the light particle at the long timescale, we need to incorporate another stochastic process into the model. The diffusing diffusivity model [24] in which the diffusion coefficient obeys the Langevin equation would be employed to incorporate the fluctuation of the speed. Some analytical results of the gas kinetic theory [25] can be utilized to design the stochastic process for the speed of the particle.

IV. CONCLUSION

In this work, we theoretically analyzed the dynamics of a light particle in heavy gas particles with large mass contrast, based on the dilute Lorentz gas model. We derived the analytical expressions for the MSD and NGP of the Lorentz gas for a given speed v . The result does not exhibit the Brownian yet non-Gaussian diffusion observed in the binary gas mixtures with mass and fraction contrast. We found that such a Brownian yet non-Gaussian diffusion can be reproduced through the ensemble average of statistical quantities of the Lorentz gas over the initial speed, except for the very long time region. This work revealed a relation between the conventional Lorentz gas and the binary gas mixture, and it will provide fresh insight into the theoretical modeling for gas diffusion.

ACKNOWLEDGMENTS

FN was supported by Grant-in-Aid for JSPS (Japan Society for the Promotion of Science) Fellows (Grant No. JP21J21725).

-
- [1] S. Chapman and T. G. Cowling, *The Mathematical Theory of Non-uniform Gases: an Account of the Kinetic Theory of Viscosity, Thermal Conduction and Diffusion in Gases*, 3rd ed. (Cambridge University Press, 1990).
 - [2] J. Jeans, *The Dynamical Theory of Gases* (Cambridge University Press, 1904).
 - [3] G. F. Mazenko, *Nonequilibrium Statistical Mechanics* (John Wiley & Sons inc, 2008).
 - [4] J. R. Dorfman, H. van Beijeren, and T. R. Kirkpatrick, *Contemporary Kinetic Theory of Matter* (Cambridge University Press, 2021).
 - [5] F. Nakai, Y. Masubuchi, Y. Doi, T. Ishida, and T. Uneyama, Phys. Rev. E **107**, 014605 (2023).
 - [6] F. Rusciano, R. Pastore, and F. Greco, Phys. Rev. Lett. **128**, 168001 (2022).
 - [7] T. Miyaguchi, Phys. Rev. E **96**, 042501 (2017).
 - [8] T. Uneyama, T. Miyaguchi, and T. Akimoto, Phys. Rev. E **92**, 032140 (2015).
 - [9] J. Kim, C. Kim, and B. J. Sung, Phys. Rev. Lett. **110**, 047801 (2013).
 - [10] J. Guan, B. Wang, and S. Granick, ACS nano **8**, 3331 (2014).
 - [11] B. Wang, S. M. Anthony, S. C. Bae, and S. Granick, Proc. Nat. Acad. Sci. **106**, 15160 (2009).
 - [12] W. He, H. Song, Y. Su, L. Geng, B. J. Ackerson, H. Peng, and P. Tong, Nat. Commun. **7**, 1 (2016).
 - [13] J.-H. Jeon, M. Javanainen, H. Martinez-Seara, R. Metzler, and I. Vattulainen, Phys. Rev. X **6**, 021006 (2016).
 - [14] K. C. Leptos, J. S. Guasto, J. P. Gollub, A. I. Pesci, and R. E. Goldstein, Phys. Rev. Lett. **103**, 198103 (2009).
 - [15] H. Kurtuldu, J. S. Guasto, K. A. Johnson, and J. P. Gollub, Proc. Nat. Acad. Sci. **108**, 10391 (2011).
 - [16] J. Machta and R. Zwanzig, Phys. Rev. Lett. **50**, 1959 (1983).
 - [17] K. Andersen and K. E. Shuler, J. Chem. Phys. **40**, 633 (1964).
 - [18] J. L. Lebowitz and H. Spohn, J. Stat. Phys. **19**, 633 (1978).
 - [19] R. Klages, S. S. G. Gallegos, J. Solanpää, M. Sarvilahti, and E. Räsänen, Phys. Rev. Lett. **122**, 064102 (2019).

- [20] M. Zeitz, K. Wolff, and H. Stark, *Eur. Phys. J. E* **40**, 1 (2017).
- [21] C. Bruin, *Physica* **72**, 261 (1974).
- [22] S. Leitmann and T. Franosch, *Phys. Rev. Lett.* **118**, 018001 (2017).
- [23] D. R. Cox and V. Isham, *Point processes*, Vol. 12 (CRC Press, 1980).
- [24] A. V. Chechkin, F. Seno, R. Metzler, and I. M. Sokolov, *Phys. Rev. X* **7**, 021002 (2017).
- [25] M. Pagitsas, J. T. Hynes, and R. Kapral, *J. Chem. Phys* **71**, 4492 (1979).